JCSE The Journal of Corrosion Science and Engineering

21st Century Corrosion Science

Volume 6 Paper C133

Effect of Drying Temperature on Chromate Conversion Coatings on Zinc

X. Zhang[1], C. van den Bos[1], W.G. Sloof[1], H. Terryn[2], A. Hovestad[3] and J.H.W. de Wit[1,2]

[1]Department of Materials Science and Technology, Delft University of Technology, Rotterdamseweg 137, 2628 AL Delft, The Netherlands

[2]Netherlands Institute for Metals Research, Rotterdamseweg 137, P.O. Box 5008, 2600 GA Delft, The Netherlands

[3]TNO Institute of Industrial Technology, P.O. Box 6235, 5600 HE Eindhoven, The Netherlands

Abstract

The effect of drying temperature on chromate conversion coatings on zinc has been studied using electrochemical impedance spectroscopy (EIS) and potentiodynamic measurements combined with FTIR and XPS surface analytical techniques. The chromate coatings were generated on pure zinc specimens in a solution (pH 1.2) containing dichromate anions and sulphuric acid at room temperature. The coatings were dried at three different temperatures: 60, 110 and 210 °C. The results show that the drying temperature not only affects the morphology of the layer, but also changes the chromium oxidation states in the layer. The coatings dried at 60 °C showed passivity, but the coatings dried at 110 °C had the fewest cracks and the highest corrosion resistance. Drying at higher temperatures (210 °C) degrades the chromate coatings by widening the cracks and reducing soluble Cr(VI) in the chromate layer. The thermal reduction of Cr(VI), detected by XPS, is probably responsible for the decrease of the Cr(VI) content of the coating.

Keywords: Chromate conversion coating, Corrosion, Electrochemical impedance, XPS, Zinc

1 Introduction

Chromate conversion coatings (CCCs) have been used for protecting metals against corrosion for many years. However, the toxic nature of Cr(VI) species necessitates a search for alternatives [1]. Although a lot of research has been done and many valuable results have been obtained, the mechanism by which CCCs inhibit the corrosion of metals is still not fully understood [2-5]. An understanding of the protective mechanism of CCCs may be useful in the search for alternatives.

It is necessary to dry chromate coatings after the chromating process, because in the wet condition the coatings are liable to mechanical damage. Furthermore, the slow removal of water from the coating at ambient temperature due to evaporation can result in pore formation and poor adhesion to the underlying zinc substrate [6]. It has been reported that drying at elevated temperatures (above 50 °C) can result in the formation of brittle, cracked chromate coatings on zinc, which provide less effective corrosion protection [7]. For magnesium substrates, however, it has been reported that heating can improve the protection provided by chromate coatings [2]. A progressive decrease in the Cr(VI) content of chromate coatings on aluminum alloys with increasing heating temperature was reported by Laget *et al.* [8]. For 2024 aluminum alloy, they found that this fall in the Cr(VI) content was associated with a significant decrease in the corrosion resistance of the coating. For 1100 aluminum alloy, on the other hand, no significant change in the corrosion resistance was observed. Clearly, the effect of the drying (or heat treatment) temperature on the corrosion protection provided by chromate conversion coatings is complicated, and is strongly dependent on the nature of the metal substrate.

In this paper, the surface structure and electrochemical characteristics of chromate coatings on zinc, after drying at different temperatures, have been investigated in order to understand the influence of the

drying temperature on the corrosion performance of chromate coatings in a solution containing chloride.

2 Experimental

2.1 Conversion coating

Zinc sheets (99.95% Zn) were cut into 7.5×2.5 cm specimens for the Fourier Transform Infrared spectroscopy (FTIR) analysis, 2.0×1.6 cm specimens for the X-ray photoelectron spectroscopy (XPS) analysis and 2.0×2.0 cm specimens for electrochemical measurements. All the specimens were polished using 1 μm diamond grains as the final polishing step. The polished specimens were cleaned in acetone and ethanol for 2 minutes, sequentially. The surfaces of specimens were activated in 0.25 % HNO_3 for 30 seconds and rinsed in deionized water before the chromating treatment was performed. Chromate conversion coating was carried out in a bath containing 200 g/l $Na_2Cr_2O_7$ + 10 g/l H_2SO_4 (pH 1.2) for 10 seconds at room temperature. After the conversion treatment, the specimens were rinsed in deionized water. After drying in flowing air, these specimens were divided into three groups and dried in an oven at 60, 110 or 210°C for 30 minutes, respectively.

2.2 Morphology analysis

The surface morphology of the chromated specimens was investigated by means of SEM. The width of the microcracks was also measured using SEM.

2.3 FTIR and XPS analyses

The compositions of the chromate coatings were analyzed by FTIR. The reflection absorbance IR spectra were obtained on the Nexus™ spectrometer from Nicolet using OMNIC software. The specimen was laid on a flat sample support. The angle of incidence was 84 degrees. The detector used was a liquid nitrogen cooled MCT-B detector. The spectra were recorded in the 4000 to 400 cm^{-1} range with a resolution of 4 cm^{-1}.

The composition of the chromate layer was also analysed by XPS. The XPS analysis was carried out with a PHI 5400 ESCA using 400 Watt Mg

K_α radiation (1253.6 eV). This instrument is equipped with a Spherical Capacitor Analyser (SCA) operating with a constant pass energy value. The energy scale of the spectrometer was calibrated according to the method described by Anthony *et al.* [9]. Overview spectra were obtained in the range of 0 – 1100 eV with an analyser pass energy of 71.55 eV. The intensities of Cr 2p, O 1s, C 1s, S 2p and Zn 2p photoelectron lines were recorded separately with an analyser pass energy of 35.75 eV. The electrons emitted from the specimens were detected at an angle of 45° with respect to the specimen surface. The C 1s peak (284.8 eV) was used as a reference to correct for electrostatic charging. The X-ray satellites, present in all measured spectra as a consequence of the non-monochromatic nature of the incident X-ray beam, were removed using the relative height and displacements with respect to the height and position of the Mg K_α. In order to assess the relative amounts of the species constituting the photoelectron lines, curve fitting was performed with symmetrical Gaussian-Lorentzian peaks after smoothing of the curve and Shirley-type subtraction of the background. The number of components to be fitted to any particular spectrum was determined by choosing the fit with the minimum reduced chi-squared value (χ^2/ν), where ν is number of degrees of freedom. Cr 2p spectra were fitted for chromium in the form of Cr_2O_3 (576.3 ± 0.2 eV), $Cr(OH)_3$ or CrOOH (577.4 ± 0.2 eV) and Cr(VI) (579.2 ± 0.2 eV) in the chromate layer [10-12].

2.4 Open-circuit potential and polarization measurements

Open-circuit potential (OCP) and potentiodynamic polarization measurements were done in a cell containing a platinum counter electrode and a reference electrode (saturated calomel electrode: $E_o \approx 0.241\ V_{NHE}$). Specimens were immersed in 0.01 M NaCl solution (pH 6) for 1 hour to establish a relatively steady open-circuit potential (OCP). Polarization measurements were then obtained by scanning the potential first from OCP to -0.25 V versus OCP, then in the opposite direction to OCP and ending at +0.25V versus OCP. The scan rate was 0.167 mV/s.

2.5 Impedance measurements

Electrochemical impedance spectroscopy (EIS) measurements were carried out in 0.01 M NaCl solution after immersion for 0.5 hours at

open circuit. The counter electrode was a flat circular platinum net, parallel to the surface of the zinc specimens. The reference electrode was an Ag-AgCl/Cl^- (saturated KCl) electrode ($E_o \approx 0.197\ V_{NHE} \approx -0.044\ V_{SCE}$). The impedance response was analyzed using a Solartron 1255 frequency response analyzer coupled with a Solartron 1287 electrochemical interface in the frequency range of 60 kHz – 0.1 Hz with 10 mV a.c. amplitude versus the OCP.

3 Results

3.1 Morphology of chromate conversion coatings

Figs. 1, 2 and 3 show the SEM images for chromate-coated specimens dried at different temperatures, 60, 110 and 210 °C, respectively.

All the chromated specimens showed microcracks in the coatings. The width of the cracks, for a coating dried at 60 °C, was about 90 nm. For a coating dried at 110 °C, it was about 110 nm and for a coating dried at 210 °C, it was 300 nm. However, concerning the crack density, *i.e.* the length of crack per unit area, the coating dried at 110 °C showed the lowest crack density. The same crack densities were also observed under an optical microscope (no optical micrographs are presented here), so the formation of the microcracks cannot be attributed to the vacuum conditions inside the scanning electron microscope.

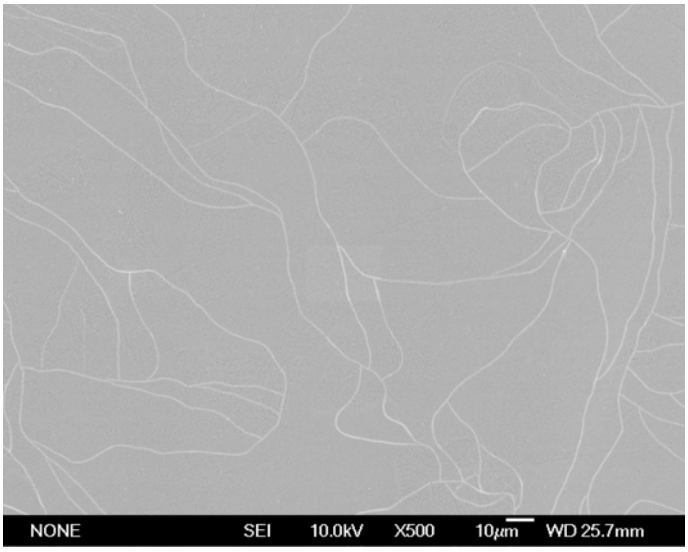

Fig. 1. SEM image for a chromate coating dried in an oven at 60°C for 30 minutes.

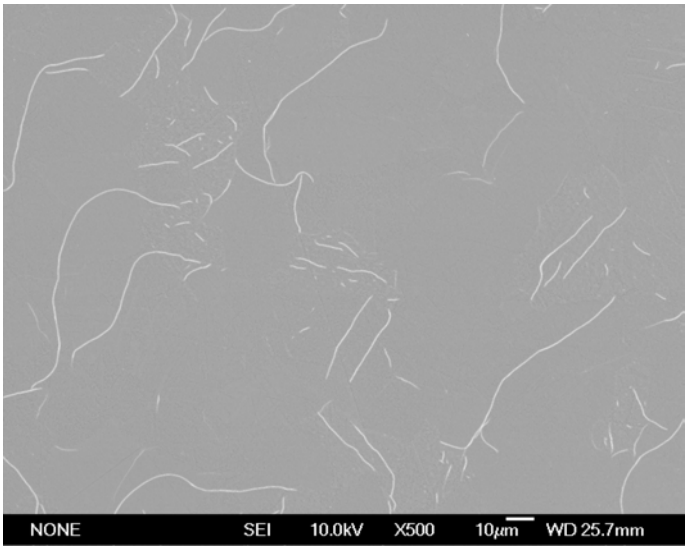

Fig. 2. SEM image for a chromate coating dried in an oven at 110°C for 30 minutes.

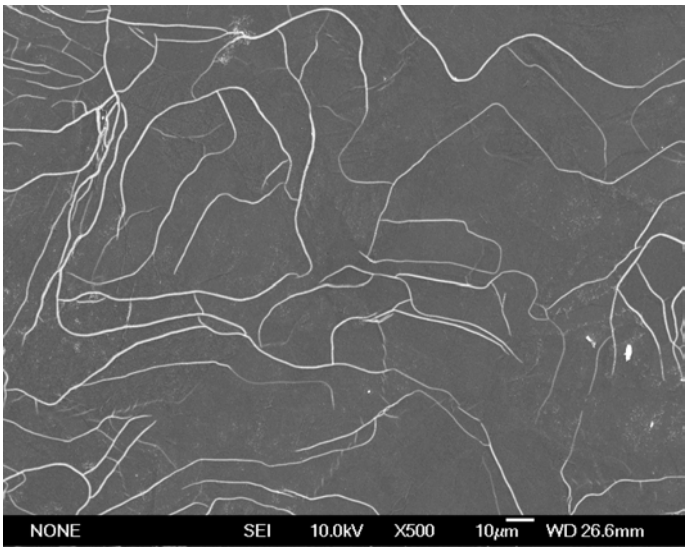

Fig. 3. SEM image for a chromate coating dried in an oven at 210°C for 30 minutes.

3.2 Thermal reduction of the Cr(VI) in the coatings

Fig. 4 shows the vibration spectra for the chromated pure zinc samples dried at 60, 110 and 210 °C. Almost all the peaks in these spectra become shorter with the increase of the drying temperature, except for the peaks in the range of 607 ~ 677 cm^{-1}.

The vibration bands around 607 and 677 cm^{-1} were attributed to Cr_2O_3. The bands between 860 and 948 cm^{-1} were attributed to the $Cr_2O_7^{2-}$ or CrO_4^{2-} anions due to the ν_1 and ν_3 vibrations, respectively

[13]. The bands between 1060 and 1126 cm^{-1} were attributed to Cr(III) compounds [14;15]. The broad absorption band observed between 3000 and 3620 cm^{-1} was attributed to water or water of hydration, and the H–O–H bending motion at 1620 cm^{-1} was also seen [16]. The peak at 1426 cm^{-1} may also be attributed to the bending vibration of water coordinated to the $Cr_2O_3 \bullet 2H_2O$ [17;18].

Fig. 4 shows that the area underneath the broad peak at 3440 cm^{-1} is smaller for the chromate coatings dried at the higher temperatures (110 and 210 °C), suggesting that the dehydration of the coating was significant for these samples. Concerning the Cr(VI) species, it is important to observe that, for the chromate coating dried at 210 °C, the peak at 948 cm^{-1} becomes lower and narrower while the peak near 677 cm^{-1} becomes taller than for the sample dried at 60 °C. For the specimen dried at 110 °C, both peaks become lower than for the sample dried at 60 °C. These changes suggest that a certain fraction of Cr(VI) species is transferred to Cr(III) compounds when the specimen is dried at a higher temperature.

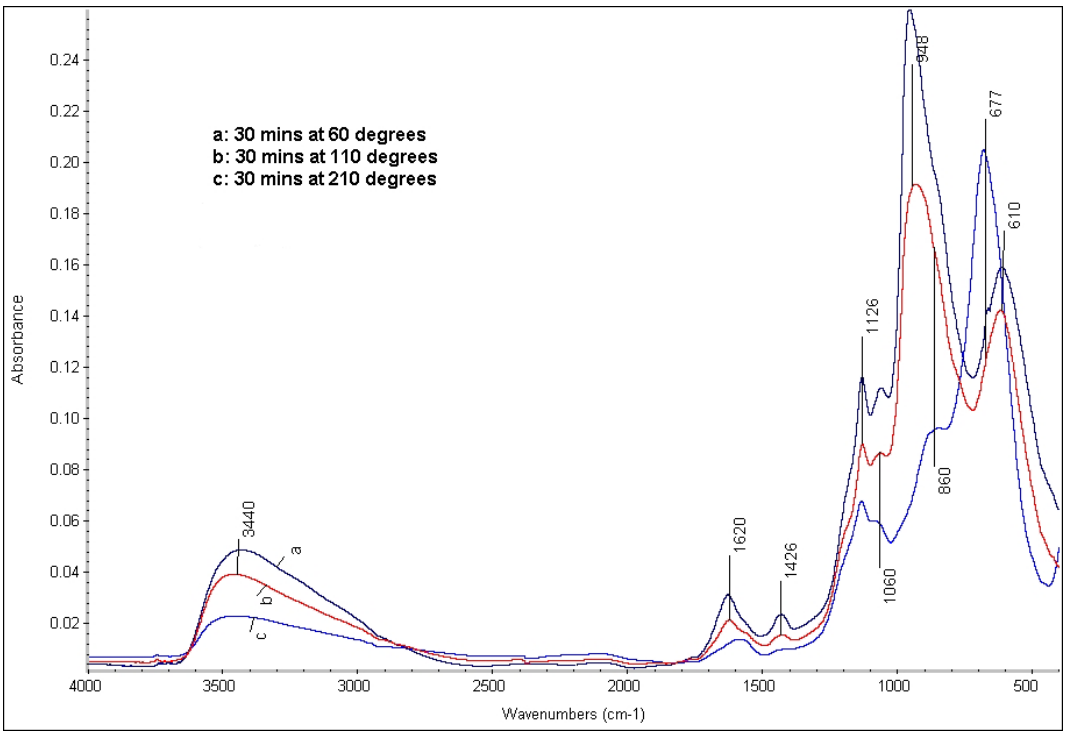

Fig. 4. FTIR vibration spectra for three chromated pure zinc samples: (a) dried at 60 °C, (b) 110 °C and (c) 210 °C for 30 minutes.

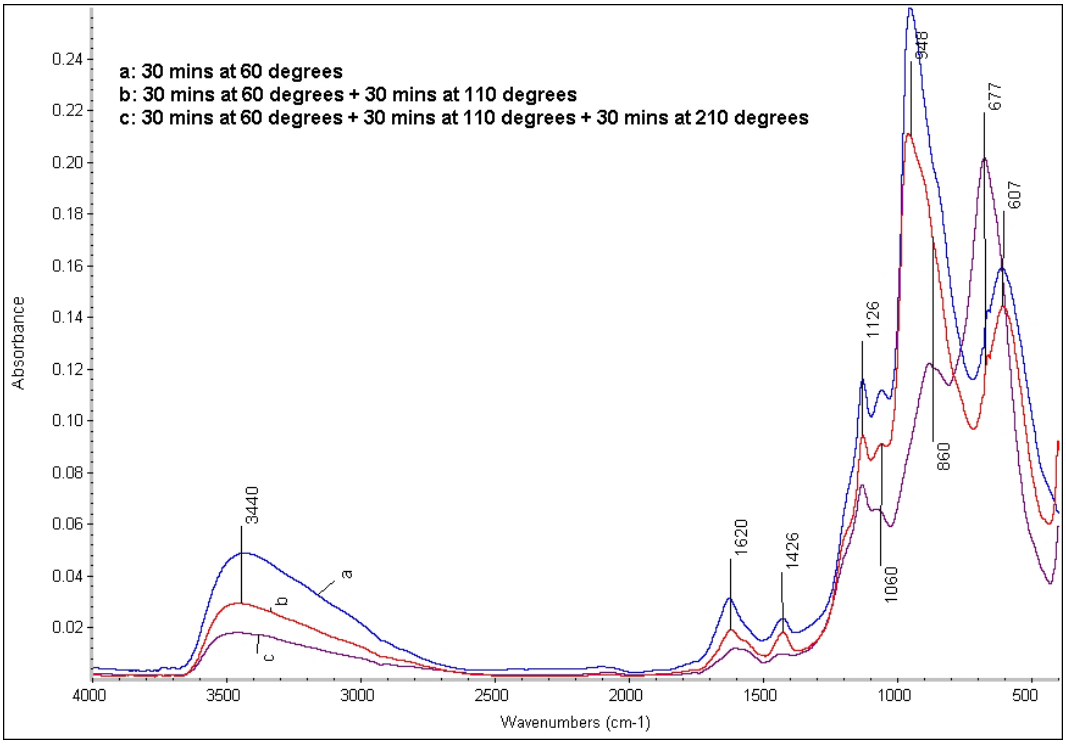

Fig. 5. FTIR vibration spectra obtained from a single chromated pure zinc sample sequentially dried at: (a) 60, (b) 110 and (c) 210 °C for 30 minutes at each temperature.

Fig. 5 shows the vibration spectra obtained from a single chromated pure zinc sample sequentially dried at 60, 110 and 210 °C for 30 minutes at each temperature. Again, dehydration with an increase of temperature was observed. The peak at 948 cm^{-1} becomes shorter and the peaks near 677 cm^{-1} become taller, again showing that a certain fraction of Cr(VI) species has been transferred to Cr(III) compounds after drying at higher temperatures.

Fig. 6 shows an XPS spectrum for a chromate coating dried at 60°C. It shows the presence of C, O, Cr, Zn and S in the top layer of the coating. When the drying temperature was increased, the carbon and zinc signals also increased (the relevant figure is not presented here), while the oxygen signal decreased. Of course, the oxidation of zinc would result in an increase of the oxygen content. However due to the dehydration of the chromate layer the net result is a loss of oxygen.

Fig. 7 shows the Cr 2p XPS spectra for chromate coatings dried at different temperatures. The peak at 579.2 eV is attributed to Cr(VI). This peak becomes shorter for the coatings dried at higher

temperatures. By increasing the drying temperature from 60 to 110 and 210 °C, the ratio of Cr(VI) to total chromium in the coating decreased from 35% to 32% and 12%, respectively.

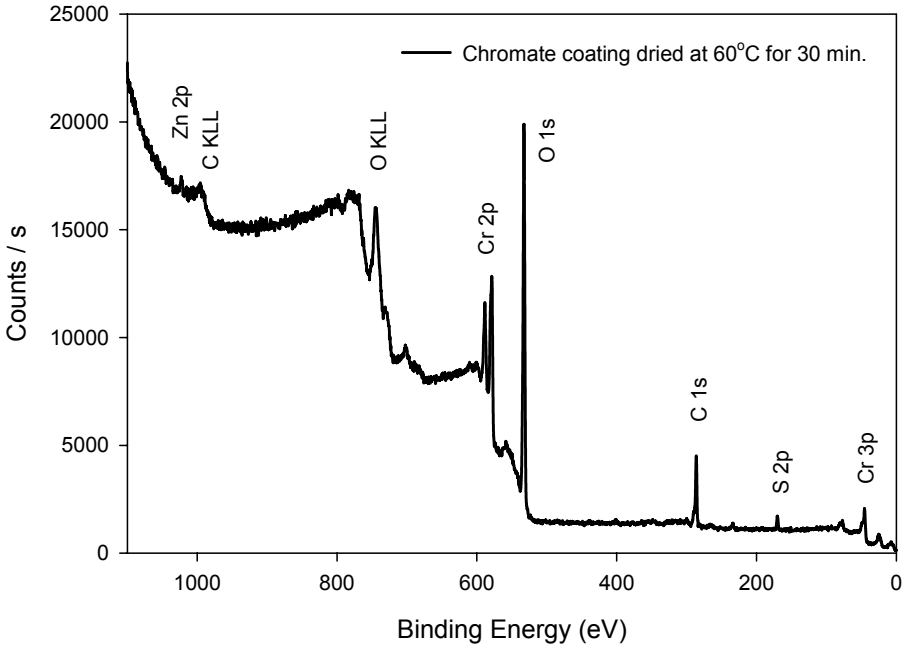

Fig. 6. XPS spectrum for a chromate coating dried at 60°C.

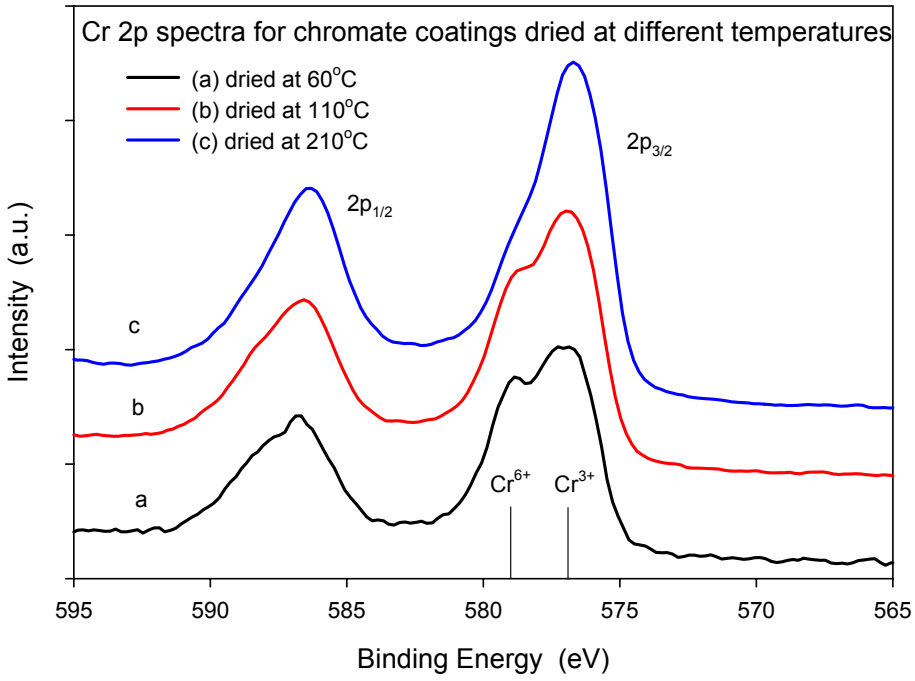

Fig. 7. Cr 2p XPS spectra for chromate coatings dried at different temperatures.

3.3 Corrosion resistance

Fig. 8 shows the polarization curves obtained in aerated 0.01 M NaCl solution, for three chromate-coated specimens all dried at 60 °C. The mixed potential moved about 120 mV in the negative direction against the OCP. All of the specimens showed a kind of anodic passivation behaviour in a range of 160 mV. The polarization curves display a good degree of reproducibility.

Fig. 9 shows the polarization curves obtained in the same corrosive medium for coatings dried at the three different temperatures. For all the coatings, the anodic breakdown potential was almost the same, around –0.92 V_{SCE}. Only for the coating dried at 60 °C did the mixed potential move in the negative direction against the OCP. Significantly, the cathodic current recorded near the OCP was smaller for the coatings dried at 110 °C than for the coatings dried at the lowest temperature (60 °C). For the chromate coatings dried at the highest temperature (210 °C), the cathodic current measured near the mixed potential was larger than for the coatings dried at 60 °C.

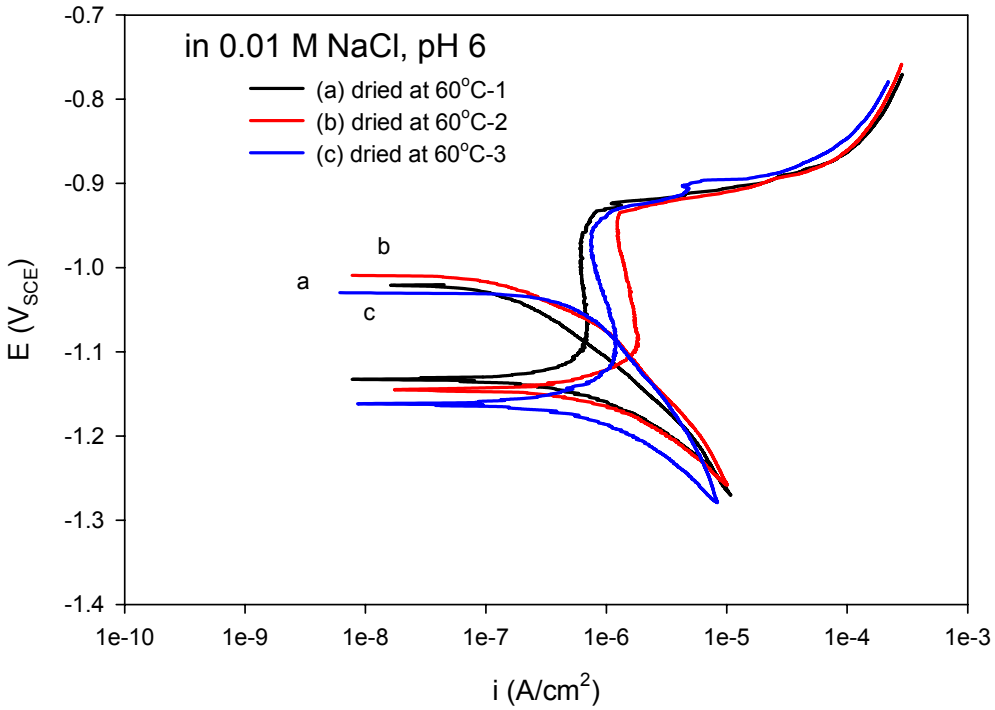

Fig. 8. Polarization curves for three chromate coated specimens dried at 60 °C. The potential scan rate was 0.167 mV/s.

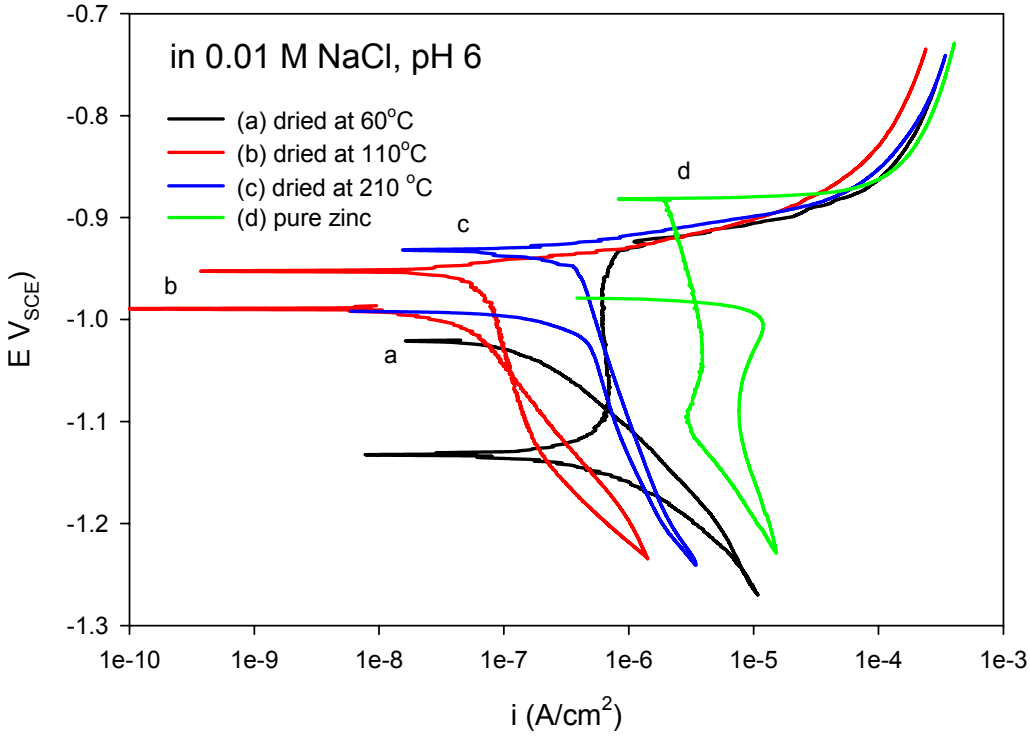

Fig. 9. Polarization curves for chromate coatings dried at different temperatures. The potential scan rate was 0.167 mV/s.

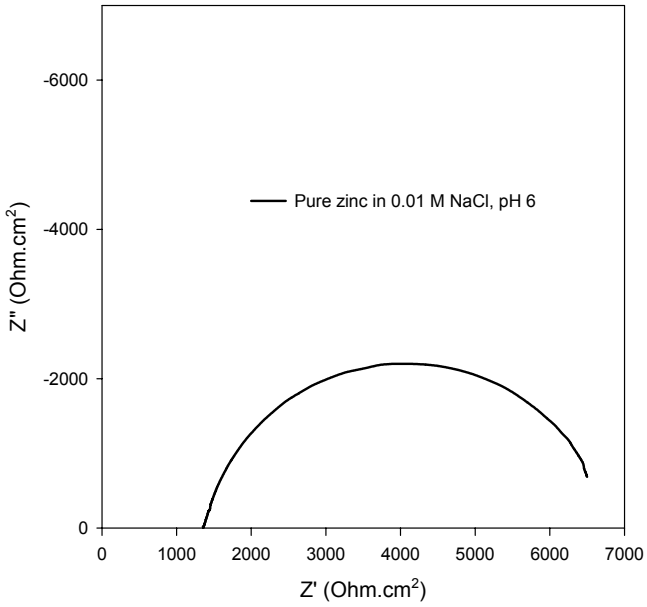

Fig. 10. The Nyquist impedance plot for non-chromated pure zinc in aerated 0.01 M NaCl solution (pH 6).

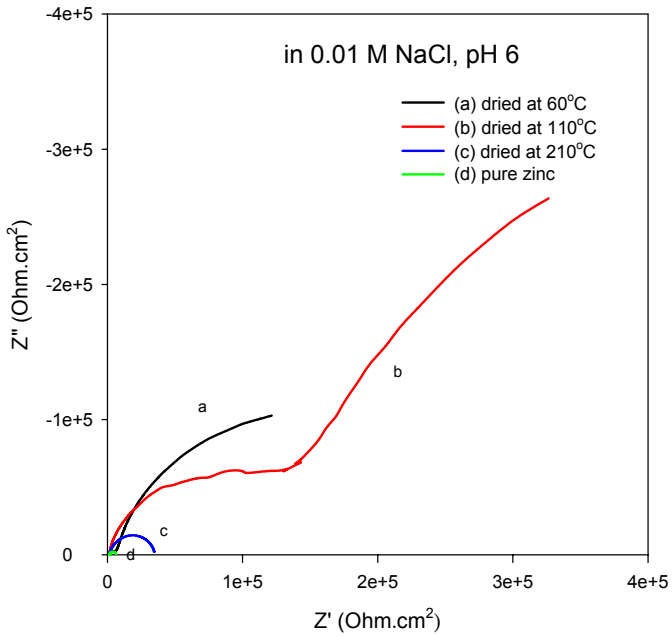

Fig. 11. The Nyquist impedance plots for the coatings dried at different temperatures.

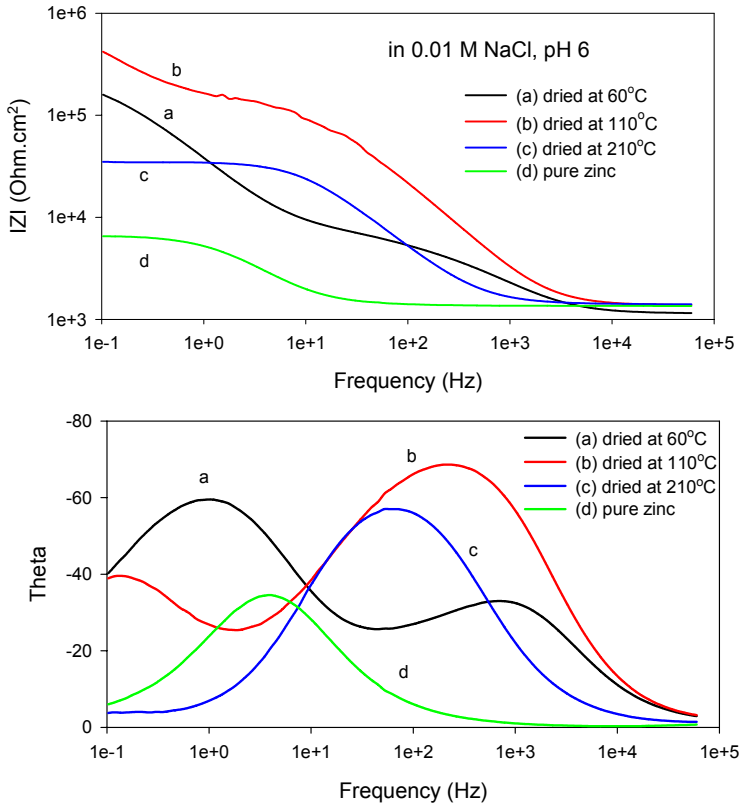

Fig. 12. The Bode impedance plots for the coatings dried at different temperatures.

Fig. 10 shows a Nyquist impedance diagram for a pure zinc specimen (with no chromate coating) in aerated 0.01 M NaCl solution (pH 6). It shows that zinc corrosion is charge transfer controlled dissolution in the NaCl solution. The charge transfer resistance is about 5.5 $k\Omega \bullet cm^2$ in this case.

Fig. 11 shows the Nyquist plots of impedance for the coatings dried at different temperatures. For the coatings dried at 60 and 110 °C, two capacitive loops were observed, while for the coatings dried at 210 °C, only one capacitive loop was observed. The capacitive loop at high frequencies is related to the chromate layer and the loop observed at lower frequencies is related to the double layer at the zinc/electrolyte interface [19].

Fig. 12 shows the Bode plots of impedance for the coatings dried at different temperatures. It shows that all the chromate coatings have larger impedance than the bare zinc. However, among the chromate coatings, the coating dried at 110 °C has the largest impedance and the coating dried at 210 °C has the lowest impedance, which is consistent with the results of the polarization measurements. The phase versus frequency curves show that there are two time constants for the coatings dried at 60 and 110 °C, while for the coating dried at 210 °C and the pure zinc there is only one time constant.

The larger impedance shown by the chromated specimens compared to the bare zinc can be attributed to the barrier nature of chromate coatings. The chromium hydroxides/oxides in the coatings hinder the access of anions such as chloride and oxygen to the metal [20]. Furthermore, the hydrophobicity of the chromate coatings will also hamper the access of oxygen dissolved in the solution to the zinc.

4 Discussion

The drying process hardens chromate coatings and increases the abrasive resistance of the surface [6]. However, the results presented above show that different drying temperatures have different effects on the morphology of chromate coatings on zinc and on their corrosion properties.

First, the drying process affects the morphology of the chromate coatings. Microcracks exist in all greenish chromate coatings on zinc when dried in air. Cracks in chromate coatings result from internal tensile stress initiated during the chromating process and the tensile stress increases with the thickness of the coatings [21]. During the drying process in air, the gel-like film formed is dehydrated and the film shrinks so that microcracks develop.

The chromate coatings dried at 210 °C have wider microcracks than the coatings dried at 60 and 110 °C. The corrosion current for the specimens dried at 210 °C is larger and the impedance is smaller than for the specimens dried at 60 and 110 °C. This means that drying at higher temperature (210 °C), as also suggested in literature [6], causes significant degradation of the chromate coatings. The microcracks are the weak places where corrosion can easily start [22]. The wider and deeper the cracks, the smaller the corrosion resistance will be. From the polarization measurements, the chromated specimens dried at 60 and 110 °C both have a lower corrosion current density. The impedance measurements also showed that the impedance is the largest for the specimens dried at 110 °C. This may be related to the observation that there are fewer microcracks in the coatings of the specimens dried at 110 °C, although the width of the cracks in these coatings was slightly larger than the width of the cracks in the coatings dried at 60 °C (see Figs. 1 and 2).

The drying process also affects the Cr(VI) species in the coatings. A progressive decrease of the Cr(VI)/total Cr ratio with temperature was observed by Laget *et al.* [8] for aluminum alloys. However, it has also been reported that the loss of "self-healing" effect of the chromates is mainly due to dehydration, which makes the Cr(VI) species immobile or insoluble, rather than to the reduction of Cr(VI) in the coating [2;5]. Another observation reported in literature is that the thermal effect on the corrosion resistance of chromate coatings depends on the substrate. Laget *et al.* attributed the fact that heating treatments do not affect the corrosion resistance of chromate coatings on Al-1100 alloy to the good corrosion resistance of the relatively pure aluminum substrate [8]. Gallaccio *et al.* observed that, in salt-fog tests, heating chromate coatings on electroplated zinc to above 75 °C resulted in

marked damage, but conversely that heating chromate coatings on magnesium improves the protection provided by the coatings [2].

In our case, Fourier Transform Infrared Spectrometry and XPS analyses of the chromate coatings have shown that the relative ratio of Cr(VI)-O species to Cr(III)-O compounds decreases after drying at higher temperatures. It means that the drying process does indeed cause Cr(VI) to be reduced to Cr(III). The polarisation curves obtained on the chromate coatings dried at 60 °C suggest that a kind of anodic passivation behaviour exists in a range of 160 mV, and all of the chromated specimens, independent of the drying temperature, showed approximately the same anodic breakdown potential, -0.92 V_{SCE}. All of the chromated specimens showed a more negative corrosion potential than the uncoated zinc in the 0.01 M NaCl solution, suggesting that this kind of conversion coating has a cathodic inhibitive effect on the corrosion of zinc: the corrosion rate of zinc is controlled by the cathodic reaction. For the coatings dried at 110 °C, the ratio of Cr(VI)/total Cr did decrease with respect to the ratio for the coatings dried at 60 °C, but this reduction was small and was not significant enough to have a negative effect on the corrosion behaviour of the coated specimens.

According to Mansfeld, the high electrochemical impedance values of chromate conversion coatings are only of secondary importance, and the corrosion protection is mainly provided by mobile Cr(VI), which inhibits the initiation and propagation of pits (for example during salt spray tests) [23]. Buchheit *et al.* reported a correlation between salt spray test results and electrochemical impedance measurements, but chromate conversion coatings can pass salt spray tests with comparatively low coating resistance values [24], again indicating that active protection resulting from the presence of mobile Cr(VI) in the coating is probably more important.

5 Conclusions

The results presented in this paper show that the temperature at which chromate coatings on zinc are dried affects not only the coating morphology, but also changes the chromium oxidation states in the

coating. All of the chromate coatings investigated in this study showed microcracks in the layer. The width of these cracks increased with the drying temperature. The coatings dried at 60 °C showed passivity, but the corrosion resistance was not the highest. Drying at a moderate temperature (110 °C) appeared to increase the corrosion resistance with respect to drying at 60 °C. However, drying at higher temperatures (210 °C) degraded the chromate coatings by widening the cracks and reducing the mobility of the soluble Cr(VI) species. The thermal reduction of Cr(VI), detected by FTIR and XPS, is probably responsible for the decrease of the Cr(VI) content of the layer. Thus, drying makes chromate coatings hard, but on the other hand, it reduces the self-healing effect of the soluble chromates.

Acknowledgements

This research was supported by the Dutch Ministry of Economic Affairs (innovation-directed research program Milieutechnologie/Zware Metalen, project number IZW 98102).

References

!ref1 G. D. Wilcox and J. A. Wharton, Trans IMF, 75, ppB140-B142, 1997.

!ref2 A. Gallaccio, F. Pearlstein, and M. R. D'Ambrosio, Metal Finishing, 8, pp50-54, 57, 1966.

!ref3 G. O. Ilevbare and J. R. Scully, J. Electrochem. Soc., 148, ppB196-B207, 2001.

!ref4 M. Kendig and S. Jeanjaquet, J. Electrochem. Soc., 149, ppB47-B51, 2002.

!ref5 V. Laget, H. S. Isaacs, C. S. Jeffcoate, and R. G. Buchheit. Thermally induced degradation of chromate conversion coatings on aluminum alloy 2024-T3. ed. Terryn, H. [2nd International symposium on aluminum surface science and technology proceedings], pp295-300, 2000. UMIST, Manchester, England, UK.

!ref6 T. Biestek and J. Weber, Conversion Coatings, Portcullis Press Ltd., Redhill, 1976.

!ref7 M. E. Roper, Metal Finishing Journal, 14, pp286-289,294, 1968.

!ref8 V. Laget, C. Jeffcoate, H. S. Isaacs, and R. G. Buchheit. Thermal stability and aging characteristics of chromate conversion coatings on aluminum alloy 2024-T3. ed. Shifler, D. A., Natishan, P. M., Tsuru, T., and Ito, S., Corrosion and corrosion control in saltwater environments, Proc. of The electrochemical society, USA, 99-26, pp173-182. 2000.

!ref9 M. T. Anthony and M. P. Seah, Surf. Interface Anal., 6, pp95-106, 1984.

!ref10 A. E. Hughes and R. J. Tayor, Surf. Interface Anal., 25, pp223-234, 1997.

!ref11 J.-O. Nilsson, S.-E. Hörnström, E. Hedlund, H. Klang, and K. Uvdal, Surf. Interface Anal., 19, pp379-385, 1992.

!ref12 B. S. Norgren, M. A. J. Somers, W. G. Sloof, and J. H. W. de Wit. The passive film on Fe-Cr alloys formed in sulphuric acid studied by voltammetry and XPS, in 12th Scandinavian Corrosion Congress & Eurocorr '92, pp139-149, 1992.

!ref13 M. Lenglet, F. Petit, and J. Y. Malvaut, Phys. Stat. Sol. (a), 143, pp361-365, 1994.

!ref14 M. Handke, A. Stoch, S. Sulima, P. L. Bonora, G. Busca, and V. Lorenzelli, Mater. Chem., 7, pp7-18, 1982.

!ref15 F. Petit, H. Debontride, M. Lenglet, G. Juhel, and D. Verchere, Appl. Spectroscopy, 49, pp207-210, 1995.

!ref16 R. A. Nyquist and R. O. Kagel, Infrared spectra of inorganic compounds, Academic Press, Inc, New York, 1971.

!ref17 P. Campestrini, S. Bohm, T. Schram, H. Terryn, and J. H. W. de Wit, Thin Solid Film, 410, pp76-85, 2002.

!ref18 J. T. Vandeburg, D. G. Anderson, J. K. Duffer, J. M. Julian, R. W. Scott, T. M. Sutliff, and M. J. Vaickus, An infrared spectroscopy atlas for the coatings industry, Philadelphia, Pennsylvania, 1980.

!ref19 L. Fedrizzi, L. Ciaghi, P. L. Bonora, R. Fratesi, and G. Roventi, J. Appl. Electrochem., 22, pp247-254, 1992.

!ref20 S. Turgoose, in B.G.Clubley (Ed.), Chemical inhibitors for corrosion control, The Royal Society of Chemistry, Manchester, 1990.

!ref21 N. M. Martyak, Surf. Coat. Technol., 88, pp139-146, 1996.

!ref22 N. M. Martyak, J. E. McCaskie, and L. Harrison, Metal Finishing, 94, pp65-67, 1996.

!ref23 F. Mansfeld, Corrosion, 54, pp595-597, 1998.

!ref24 R. G. Buchheit, M. Cunningham, H. Jensen, M. W. Kendig, and M. A. Martinez, Corrosion, 54, pp 61-72, 1998.